

Lipid nanoparticle-encapsulated DNA vaccine robustly induce superior immune responses to the mRNA vaccine in Syrian hamsters

Hung-Chun Liao,^{1,4} Kuan-Yin Shen,^{1,4} Chung-Hsiang Yang,¹ Fang-Feng Chiu,¹ Chen-Yi Chiang,¹ Kit Man Chai,¹ Wan-Chun Huang,¹ Hui-Min Ho,¹ Yi-Hua Chen,¹ Min-Syuan Huang,¹ Ching-Len Liao,¹ Hsin-Wei Chen,^{1,2,3} Ming-Hsi Huang,^{1,2,3} and Shih-Jen Liu^{1,2,3}

¹National Institute of Infectious Diseases and Vaccinology, National Health Research Institutes, Miaoli, Taiwan; ²Graduate Institute of Biomedical Sciences, China Medical University, Taichung, Taiwan; ³Graduate Institute of Medicine, College of Medicine, Kaohsiung Medical University, Kaohsiung, Taiwan

DNA vaccines for infectious diseases and cancer have been explored for years. To date, only one DNA vaccine (ZyCoV-D) has been authorized for emergency use in India. DNA vaccines are inexpensive and long-term thermostable, however, limited by the low efficiency of intracellular delivery. The recent success of mRNA/lipid nanoparticle (LNP) technology in the coronavirus disease 2019 (COVID-19) pandemic has opened a new application for nucleic acid-based vaccines. Here, we report that plasmid encoding a trimeric spike protein with LNP delivery (pTS/LNP), similar to those in Moderna's COVID-19 vaccine, induced more effective humoral responses than naked pTS or pTS delivered via electroporation. Compared with TSmRNA/LNP, pTS/LNP immunization induced a comparable level of neutralizing antibody titers and significant T helper 1-biased immunity in mice; it also prolonged the maintenance of higher antigen-specific IgG and neutralizing antibody titers in hamsters. Importantly, pTS/LNP immunization exhibits enhanced cross-neutralizing activity against severe acute respiratory syndrome coronavirus 2 (SARS-CoV-2) variants and protects hamsters from the challenge of SARS-CoV-2 (Wuhan strain and the Omicron BA.1 variant). This study indicates that pDNA/LNPs as a promising platform could be a next-generation vaccine technology.

INTRODUCTION

The coronavirus disease 2019 (COVID-19) pandemic is caused by severe acute respiratory syndrome coronavirus 2 (SARS-CoV-2) and its rapidly evolving variants. Although numerous COVID-19 vaccines have been used in humans, the rapid mutation of the virus causes current vaccines to become ineffective. Nucleic acid vaccines, such as mRNA or DNA vaccines, could be developed in a short period, allowing for a rapid response to emerging infectious disease outbreaks. In storage, DNA vaccines are more stable than mRNA vaccines, making them easier to distribute to developing countries. Furthermore, the rapid mass production of DNA vaccines can result in the production of a vaccine for circulating COVID-19 variants. However, the most significant obstacle that DNA vaccines must overcome is the lack of

an effective delivery system. DNA vaccines have been delivered using a variety of methods, including liposomes,^{1,2} polymers,^{3–5} needle-free biojets,^{6,7} and electroporation.^{8–10} The majority of COVID-19 DNA vaccines are still in clinical trials, and only one DNA vaccine (ZyCoV-D) has received COVID-19 emergency use authorization in India.^{11,12} However, the low efficacy (66.6%) of ZyCoV-D indicated that the efficacy of next-generation DNA vaccines needs to be improved. Many researchers are currently using electroporation to deliver DNA vaccines. Because DNA vaccines delivered by electroporation are highly efficient, this approach can induce strong humoral and cellular immune responses against SARS-CoV-2.^{13–15} However, the disadvantage of electroporation is that it necessitates the use of an electric device, which is inconvenient and must be approved by regulatory authorities. Although electroporation of DNA vaccines may be useful for vaccination in a small population, it is difficult to apply to mass vaccinations. Thus, there remains a need for the development of effective and easily administered DNA vaccines.

The viral DNA delivery system is highly efficacious and has been utilized in clinical studies for a long time.^{16–18} In addition, adenovirus-delivered DNA vaccines against COVID-19 have been approved, including chimpanzee adenovirus (AstraZeneca),^{19,20} human adenovirus type 5 (CanSino),^{21,22} and type 26 (Janssen).^{23,24} However, a limitation exists regarding the development of anti-viral vector antibodies, which reduces booster efficacy.²⁵ In this field, non-viral delivery systems for DNA vaccines are becoming more compelling. Nanoparticles (NPs) are typically less than 200 nm in size, which makes them a promising nonviral delivery system for

Received 14 June 2023; accepted 30 November 2023;
<https://doi.org/10.1016/j.omtm.2023.101169>.

⁴These authors contributed equally

Correspondence: Ming-Hsi Huang, National Institute of Infectious Diseases and Vaccinology, National Health Research Institutes, Miaoli, Taiwan.

E-mail: huangminghsi@nhri.edu.tw

Correspondence: Shih-Jen Liu, National Institute of Infectious Diseases and Vaccinology, National Health Research Institutes, Miaoli, Taiwan.

E-mail: levent@nhri.edu.tw



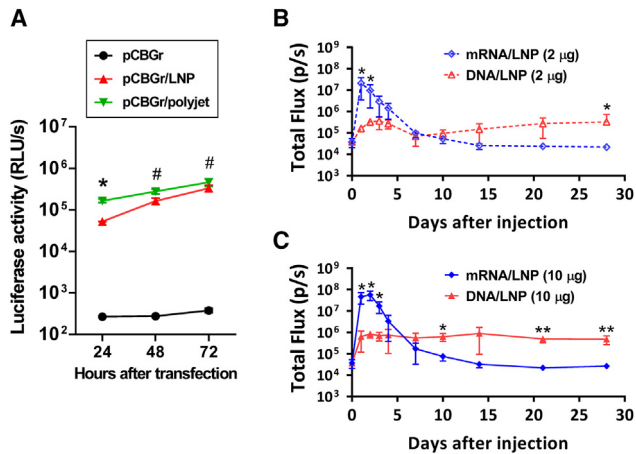


Figure 1. LNP delivery facilitates pDNA-encoded protein expression *in vitro* and *in vivo*

(A) The 293T cells were incubated with 2 µg CBGr99-expressing plasmid (pCBGr), either naked plasmid, encapsulated by LNP or polyjet for 72 h. The relative light units (RLUs) measured by spectrum meter represent the luciferase activity expressed from the indicated combinations, respectively. (B and C) BALB/c mice ($n = 4/\text{group}$) were i.m. injected with 2 µg and 10 µg CBGr99 encoding mRNA or pDNA. The luciferase activities that derived from CBGr99 expression at the injected sites on mice were monitored by IVIS at the indicated time points. The p value was calculated by two-way ANOVA, * $p < 0.05$, ** $p < 0.005$, # not significant.

a wide range of applications.²⁶ In particular, liposomal or polymeric NPs can encapsulate DNA or small nucleic acids that can then be used in vaccines or therapeutics.^{27,28} Although NPs have been developed for many years, no successful products were released to the market until lipid NPs (LNPs) were used in mRNA and small interfering RNA products.^{28,29} LNPs are similar to NPs, but contain an ionizable lipid that allows mRNA to be released into the cytosol.^{30,31} The successful use of LNPs in RNA products could be extended to DNA products. Nonetheless, the formulation of LNPs for DNA may differ from that of mRNA. Some new LNP formulations for DNA delivery have been tested.^{32–34} Based on their LUNAR technology (Arcturus Therapeutics), Mucker et al.³⁵ used LNPs formulated with the Andes virus or Zika virus DNA vaccines. In comparison with DNA alone vaccination, administration of DNA/LNPs can elicit the production of a 10-fold increased neutralizing antibody titer in rabbits and nonhuman primates.

Here, the LNPs with the formulations same as COVID-19 vaccines from Moderna can also be used to efficiently deliver circular plasmid DNA into cells for expression of the encoded proteins. Additionally, we found that immunization with SARS-CoV-2 spike-encoding DNA/LNPs robustly induces spike-specific antibody production in various species (mouse, rat, rabbit, and hamster), which is particularly higher than mRNA/LNPs in hamsters. The neutralizing antibody titers were sustained for 20 weeks after immunization with DNA/LNPs, but not with mRNA/LNPs. Hamsters immunized with DNA/LNP induced immune responses against challenge with SARS-CoV-2 (Wuhan strain and Omicron variant BA.1) and enhanced cross-

neutralizing activity against BA.5 over mRNA/LNP. These studies showed that DNA/LNPs could be a new vaccine technology for emerging infectious disease outbreaks.

RESULTS

Protein expression upon delivery of pDNA/LNPs *in vitro* and *in vivo*

To assess the plasmid DNA delivery efficiency by LNPs, 293T cells were used for transfection of plasmid DNA encoding luciferase protein (pCBGr). The luciferase activity in cell lysates was determined by luminescence measurement after incubated with 2 µg naked pCBGr, pCBGr/LNP, or pCBGr/polyjet transfection reagent for 24, 48, and 72 h. The lysates for both pCBGr/LNP and pCBGr/polyjet had high levels of luciferase activity (Figure 1A). However, the lysate for pCBGr naked DNA in 293T cells had only limited luciferase activity. Although the luciferase activity for pCBGr/LNP was lower than the luciferase activity for pCBGr/polyjet at 24 h, the luciferase activity for pCBGr/LNP had no significant difference compared that for pCBGr/polyjet at 48 and 72 h. This result indicated that LNP-encapsulating DNA could promote the *in vitro* expression as well as the commercial transfecting agent polyjet.

In vivo expression of DNA/LNP was compared with that of mRNA/LNP in mice injected intramuscularly at the hindlimb with 2 µg (Figure 1B) and 10 µg (Figure 1C) CBGr99-encoding pDNA or mRNA. In mice injected with 2 µg or 10 µg CBGr mRNA/LNP, the luminescence signals increased above 1×10^7 p/s within 24 h and then progressively decreased to background levels (3×10^4 p/s) within 7 days. In contrast, continuous moderate luminescence signals (6×10^5 p/s) were detected in mice injected with 2 or 10 µg CBGr DNA/LNP (Figure S1). The *in vivo* luminescence signals show the magnitude of luciferase expression derived by mRNA/LNP is significantly higher than DNA/LNP. Nonetheless, DNA/LNP can promote a stable and prolonged protein expression *in vivo* for at least one month.

The trimeric spike pDNA/LNP immunization induced robust humoral responses in rodents

Previously, we designed a recombinant trimeric spike (TS) expression system to increase protein yield and enhance antiviral humoral responses.³⁶ We further found the LNPs encapsulating plasmid that encodes TS (pTS) was superior to full-length S protein (pS) in producing anti-spike total IgG in mice (Figure S2A) and hamsters (Figure S2B). Moreover, either pTS/LNP or pS/LNP immunization elicited a high anti-S IgG titer in the Sprague-Dawley rat model (Figure S2C). These results demonstrated that pTS/LNP could efficiently induce the production of SARS-CoV-2 S-specific IgG in three rodent models.

To further assess whether pTS DNA/LNP immunization could induce satisfactory antiviral immunity, naked DNA and DNA delivered via electroporation were included in the comparison. BALB/c mice were immunized with pTS, pTS with EP, or pTS/LNP (2 µg or 20 µg) at a 3-week interval. Serum were collected from 3 to 12 weeks, and ELISA was used to monitor the kinetics of anti-TS IgG titers. After boosting, the anti-TS IgG titer for pTS/LNP increased from log

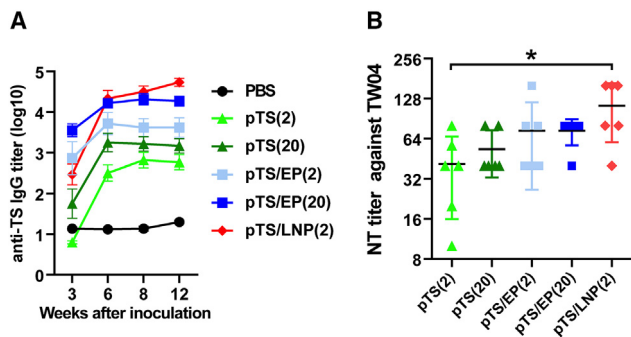


Figure 2. DNA/LNP delivery induces humoral immune responses

BALB/c mice ($n = 6/\text{group}$) were immunized with pTS DNA ($2 \mu\text{g}$ or $20 \mu\text{g}$) by direct i.m. injection, electroporation (EP), or LNP at 0 and 3 weeks. (A) The spike-specific total IgG titers of sera collected from the indicated time points were determined by antigen-coating ELISA. (B) The sera collected 12 weeks after the first vaccination was used to determine live-virus neutralization titer. The p value was calculated by Mann-Whitney test. $*p < 0.05$.

2.46 ± 0.25 at week 3 to $\log 4.33 \pm 0.2$ at week 6. The anti-TS IgG titer of the pTS/LNP group was sustained from week 6 to week 12 as well as the $20 \mu\text{g}$ pTS/EP group, but was higher than that of the $2 \mu\text{g}$ pTS/EP group or $2 \mu\text{g}$ pTS group (Figure 2A). In addition, the neutralizing antibody titer (NT titer) in serum (week 12) of the $2 \mu\text{g}$ pTS/LNP group was significantly higher than that of the $20 \mu\text{g}$ pTS/EP group (Figure 2B). These findings indicated that DNA/LNPs could represent an effective strategy for eliciting a robust humoral immune response.

TS DNA/LNP vaccination elicit stronger humoral responses than mRNA/LNP in hamsters

To extensively compare the immunogenicity of the TS DNA/LNP vaccine with the TS mRNA/LNP vaccine, which encode the same TS antigen but synthesized as mRNA and encapsulated by using the same formulation as mRNA-1273 vaccine from Moderna.³⁷ Four animal models were immunized twice at a 2-week interval with the indicated dosages of TSmRNA/LNP and pTS/LNP. In BALB/c mice, Sprague-Dawley rats, and New Zealand rabbits, the anti-TS IgG titers elevated rapidly within 2 weeks after the second vaccination of TSmRNA/LNP then decrease to a level similar to pTS/LNP, which induced an anti-TS IgG level more sustained for long-term production (Figure 3). Generally, the pTS/LNP immunization elicited anti-TS IgG production levels comparable with TSmRNA/LNP 4 weeks after boost vaccination in these animals. Surprisingly, pTS/LNP immunization elicited significantly higher anti-TS IgG titers than TSmRNA/LNP in Syrian hamsters, which were sustained at approximately $\log 5\text{--}6$ until week 20 (Figure 3D).

We further analyzed the anti-viral activities of neutralizing antibodies induced by TSmRNA/LNP or pTS/LNP vaccination. Compared with pTS/LNP, mice immunized with TSmRNA/LNP showed a significantly higher anti-TS IgG titer at week 6 (Figure 4A), but only an equivalent neutralizing antibody titer at week 6 (Figure 4B) and week 20 (Figure 4C). However, the serum of pTS/LNP immunized hamsters had

a significantly higher level of total anti-TS IgG titers (Figure 4D) and neutralizing antibody titers (Figure 4E) than those of TSmRNA/LNP group at week 6, and the increased neutralizing antibodies in serum from the pTS/LNP group lasted until week 20 (Figure 4F). These results demonstrated that pTS/LNP immunization induced robust humoral responses, which are comparable with TSmRNA/LNP and particularly stronger than TSmRNA/LNP in hamsters.

Cellular immune responses to pTS DNA/LNP vaccination

To further characterize the T helper 1 (Th1)/Th2 immunological profile induced by different types of vaccines, BALB/c mice were immunized with $2 \mu\text{g}$ TSmRNA/LNP, pTS/LNP, or TS/alu twice at a 3-week interval. One week after the last vaccination, splenocytes were collected and re-stimulated with $5 \mu\text{g}/\text{mL}$ recombinant TS

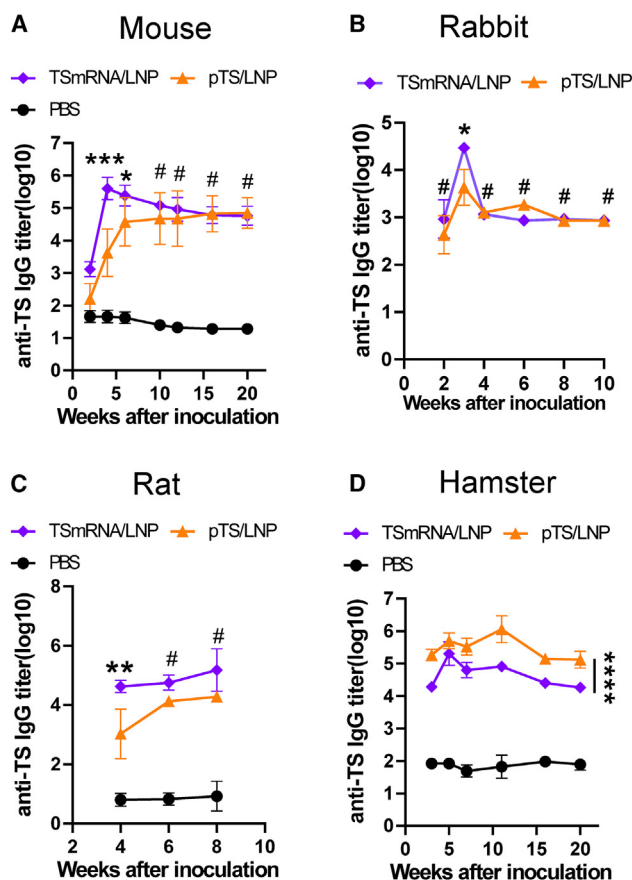


Figure 3. Comparative kinetics of anti-TS IgG titers induced by mRNA/LNP and DNA/LNP

(A) BALB/c mice ($n = 6/\text{group}$) were immunized with PBS as control, $2 \mu\text{g}$ TSmRNA/LNP, or pTS/LNP at weeks 0 and 2. (B) Rabbits ($n = 3/\text{group}$) were immunized with $50 \mu\text{g}$ TSmRNA/LNP or pTS/LNP at weeks 0 and 2. (C) Sprague-Dawley rats ($n = 4/\text{group}$) and (D) Syrian hamsters ($n = 5/\text{group}$) were immunized with PBS as control, $10 \mu\text{g}$ mRNA/LNP, or TS/LNP at weeks 0 and 2. The spike-specific IgG titer was monitored by ELISA at indicated time points from 2 to 20 weeks. The p value was calculated by two-way ANOVA. $*p < 0.05$, $**p < 0.008$, and $***p < 0.0005$. # Not significant.

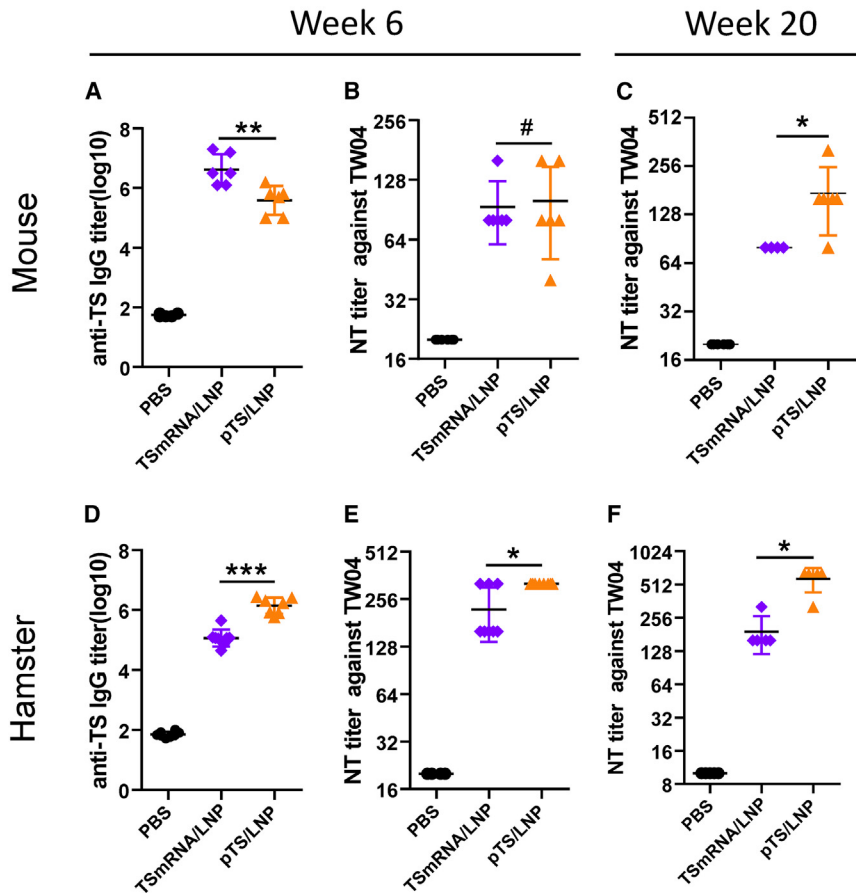


Figure 4. The pTS/LNP immunization induces robust and long-lasting neutralizing antibodies

(A–C) Balb/c mice ($n = 6/\text{group}$) were immunized with PBS as control, 2 μg TSmRNA/LNP, or pTS/LNP at weeks 0 and 2. (D–F) Syrian hamsters ($n = 8/\text{group}$) were immunized with 10 μg TSmRNA/LNP or pTS/LNP at weeks 0 and 2. The sera collected from individual animals at week 6 were used to determine (A and D) the spike-specific IgG titers by antigen-coating ELISA. The neutralizing titers were analyzed by TCID₅₀ assay at (B and E) week 6 and (C and F) week 20. The p value was calculated by Mann-Whitney test. * $p < 0.05$, ** $p < 0.008$ and *** $p < 0.0005$ were considered significant; # Not significant.

SARS-CoV-2 (Wuhan strain) to detect the viral load in the lung at 3 days post-challenge (dpc), and lung injury was evaluated by histochemistry at 6 dpc (Figure 6A). Moreover, the mean virus titers in the lungs of hamsters that received PBS, TSmRNA/LNP, or pTS/LNP were log 10, log 5, and log 1 (50% tissue culture infectious dose [TCID₅₀]/mL) at dpc 3, respectively (Figure 6B). This result indicated that pTS/LNP immunization more robustly induced virus clearance than TSmRNA/LNP immunization. Accordingly, the histochemistry analysis showed less inflammation in the lungs of TSmRNA/LNP- and pTS/LNP-immunized hamsters than in the lungs of PBS-treated hamsters (Figure 6C). The severity score for pTS/LNP immunization was zero, which was superior to that for TSmRNA/LNP immunization (Figure 6D). These results demonstrated that pTS/LNP induced robust virus inhibition immunity and protection to prevent lung injury.

protein for 72 h. The concentrations of interferon (IFN)- γ , IL-2, IL-5, and IL-13 in the splenocyte culture supernatant were determined by sandwich cytokine ELISA (Figures 5A–5D).

These results showed that splenocytes from mice receiving TS/alu produced relatively high concentrations of IFN- γ , IL-2, IL-5, and IL-13 in a Th1- and Th2-balanced manner. Compared with TS/alu as a reference, TSmRNA/LNP-immunized splenocytes could produce a similar level of Th1 cytokines (IFN- γ and IL-2) but lower levels of Th2 cytokines (IL-5 and IL-13), resulting in higher ratios of Th1/Th2 profile (Figures 5E and 5F). The levels of Th1 and Th2 cytokines detected in the TSmRNA/LNP group were statistically higher than those in the pTS/LNP group. However, pTS/LNP immunization resulted in the highest ratios of IFN- γ /IL-5 (Figure 5E) and IFN- γ /IL-13 (Figure 5F) compared with other groups, indicating a Th1-biased immune response. These results revealed that the LNP-encapsulated nucleic acid vaccine, especially the pDNA/LNP vaccine, induced a Th1-biased response.

Immune protection induced by pTS DNA/LNP against viral challenge in hamsters

To evaluate the protective effect of the pTS/LNP vaccine, hamsters were immunized with 10 μg TSmRNA/LNP or pTS/LNP at a 2-week interval. The immunized hamsters were infected with

SARS-CoV-2 (Wuhan strain) to detect the viral load in the lung at 3 days post-challenge (dpc), and lung injury was evaluated by histochemistry at 6 dpc (Figure 6A). Moreover, the mean virus titers in the lungs of hamsters that received PBS, TSmRNA/LNP, or pTS/LNP were log 10, log 5, and log 1 (50% tissue culture infectious dose [TCID₅₀]/mL) at dpc 3, respectively (Figure 6B). This result indicated that pTS/LNP immunization more robustly induced virus clearance than TSmRNA/LNP immunization. Accordingly, the histochemistry analysis showed less inflammation in the lungs of TSmRNA/LNP- and pTS/LNP-immunized hamsters than in the lungs of PBS-treated hamsters (Figure 6C). The severity score for pTS/LNP immunization was zero, which was superior to that for TSmRNA/LNP immunization (Figure 6D). These results demonstrated that pTS/LNP induced robust virus inhibition immunity and protection to prevent lung injury.

pTS DNA/LNP induces protective immunity against BA.1 variant challenge

To further assess the protective efficacy of the pTS/LNP vaccine against variant of concern (VOC) infection and associated illnesses, another spike protein from the Omicron BA.1 variant (TSomi), which contains the same modification as TS, was also included in the comparison. In this study, Syrian hamsters were immunized with 2 μg TSomi mRNA/LNP, pTSomi/LNP, or pTS/LNP twice at a 2-week interval and subsequently challenged by the SARS-CoV-2 Omicron BA.1 variant through intranasal infection (Figure 7A). Serum from each group of immunized hamsters was collected at week 6 before the viral challenge and subjected to assessment of the titers of total Omicron TS protein (TSomi)-binding IgG (Figure 7B) and the titers of neutralizing antibodies against the Omicron BA.1 variant (Figure 7C).

The mean anti-TSomi IgG titers in serum from hamsters vaccinated with the PBS control, TSomi mRNA/LNP, pTSomi DNA/LNP, or pTS/LNP were log 1.38, log 3, log 4.78, and log 4.7, respectively

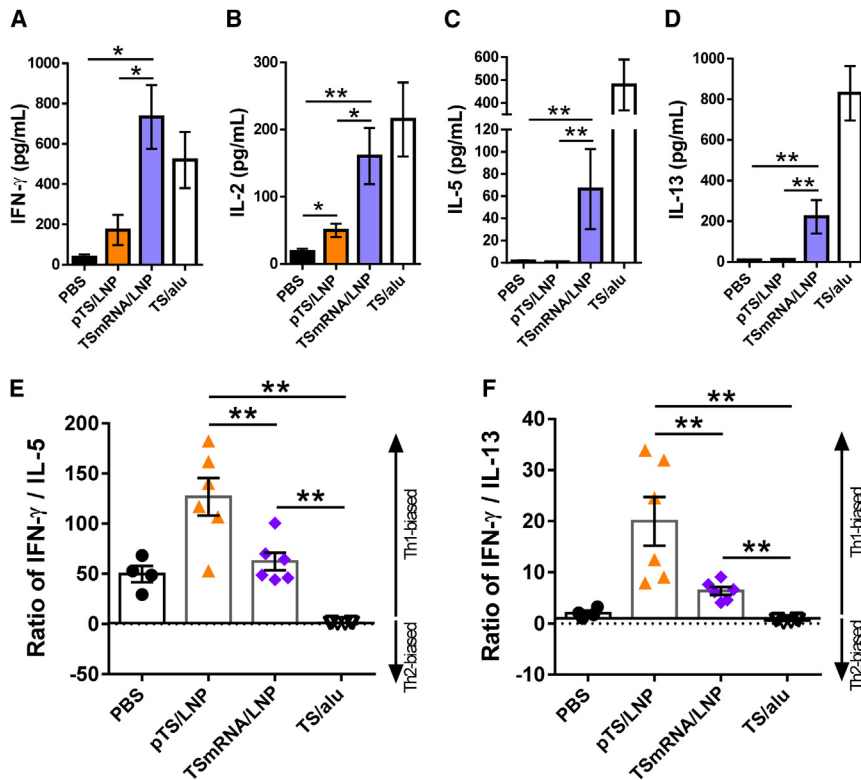


Figure 5. The pTS/LNP immunization induces Th1-bias cytokine profiles in murine

BALB/c mice ($n = 6$ /group) were immunized with PBS as control, 2 μ g TSmRNA/LNP, 2 μ g pTS/LNP, or 2 μ g TS protein formulated with 150 μ g Al(OH)₃ gel at weeks 0 and 3. The immunized mice were sacrificed at week 4 and the splenocytes were collected to re-stimulate with TS protein (5 μ g/mL) for 72 h. The cytokines (A) IFN- γ , (B) IL-2, (C) IL-5, and (D) IL-13 in the culture supernatant of indicated groups were determined by sandwich ELISA. The (E) IFN- γ /IL-5 and (F) IFN- γ /IL-13 ratios were calculated from the concentrations of IFN- γ , IL-5, and IL-13 from individual mice. A ratio of >1 represented a Th1 bias. The p value was calculated by Mann-Whitney test. ** $p < 0.008$ were considered significant.

(Figure 7B). Both the anti-TSomi IgG and BA.1-neutralizing antibody titers (Figure 7C) in the serum of the pTSomi/LNP group were remarkably higher than those of the TSomi mRNA/LNP group. Moreover, hamsters that received pTS/LNP immunization also generated anti-TSomi IgG equal to pTSomi/LNP group and BA.1-neutralizing antibodies similar to TSomi mRNA/LNP group 4 weeks after the boost vaccination.

After Omicron BA.1 variant challenge, the hamsters in the PBS control group exhibited a relatively high viral load in the lung (log 4–7 TCID₅₀/mL) at 3 dpc (Figure 7D) and significant body weight loss at 4 dpc (Figure 7E). TSomi mRNA/LNP vaccination protected hamsters from weight loss and successfully suppressed viral replication in two of four hamsters, but the other two hamsters still had a high viral load (>log 5 TCID₅₀/mL). However, the hamsters in both groups vaccinated with pTSomi DNA/LNPs or pTS/LNPs did not experience any weight loss within 6 dpc (Figure 7E) and completely controlled the viral load in their lungs below the detectable limit (Figure 7D). These data support that pTS/LNP immunization can induce protective immunity, as well as pTSomi/LNP immunization to prevent Omicron BA.1 VOC infection in hamsters.

The pDNA/LNP immunization enhances cross-neutralizing activities over mRNA/LNP in hamsters

To verify the ability of DNA/LNPs vaccines to elicit neutralizing antibodies against different SARS-CoV-2 VOCs, hamsters were immunized with 10 μ g TSmRNA/LNP, pTS/LNP, TSomi mRNA/LNP, or

pTSomi/LNP at weeks 0 and 2. Serum collected at week 6 from individual hamsters was assessed by TCID₅₀ neutralization to determine the titers of neutralizing antibodies. These results revealed that immunization of pDNA/LNP encoding either TS or TSomi induced significantly higher serum NT titers against Omicron BA.1 and BA.5 than its mRNA/LNPs (Figures 8A and 8B). To our surprise, pTS/LNP immunization induced NT titers against BA.1 that were equivalent to TSomi mRNA/LNP, whereas NT titers against BA.5 were significantly higher than TSomi mRNA/LNP.

Notably, the results of serum neutralization assay of Wuhan-TW04 showed that the pTS/LNP immunization elicited high nAb levels (mean NT titer, 320 \pm 0), which had 3.75-fold and 5.5-fold reduction compared with those against Omicron BA.1 and BA.5, respectively. However, TSmRNA/LNP-immunized hamsters had serum NT titers against Wuhan-TW04 (mean, 220 \pm 83), which were 8- and 16-fold lower in neutralizing Omicron BA.1 and BA.5, respectively. (Figures 8C and 8D). In addition, the serum NT titers of hamsters receiving TSomi mRNA/LNP or pTSomi/LNP, as measured by neutralization assay of SARS-CoV-2 Omicron BA.1, were decreased by 10.25-fold and 7.25-fold, respectively, when they measured by Omicron BA.5 neutralization (Figure 8E). Similar results were repeatedly observed from these studies, hamsters immunized with mRNA/LNP had more significant decreases in serum NT titers against different VOCs than those immunized with DNA/LNP. These findings suggest that DNA/LNP-induced neutralizing antibodies are more resistant than mRNA/LNP when they encounter variants that escape neutralization.

DISCUSSION

DNA vaccines have been continually investigated for emerging diseases due to their high thermostability and ease of manufacture. Unlike mRNA vaccines, which need to be stored at an ultralow temperature, DNA vaccines can be stored at room temperature for 1

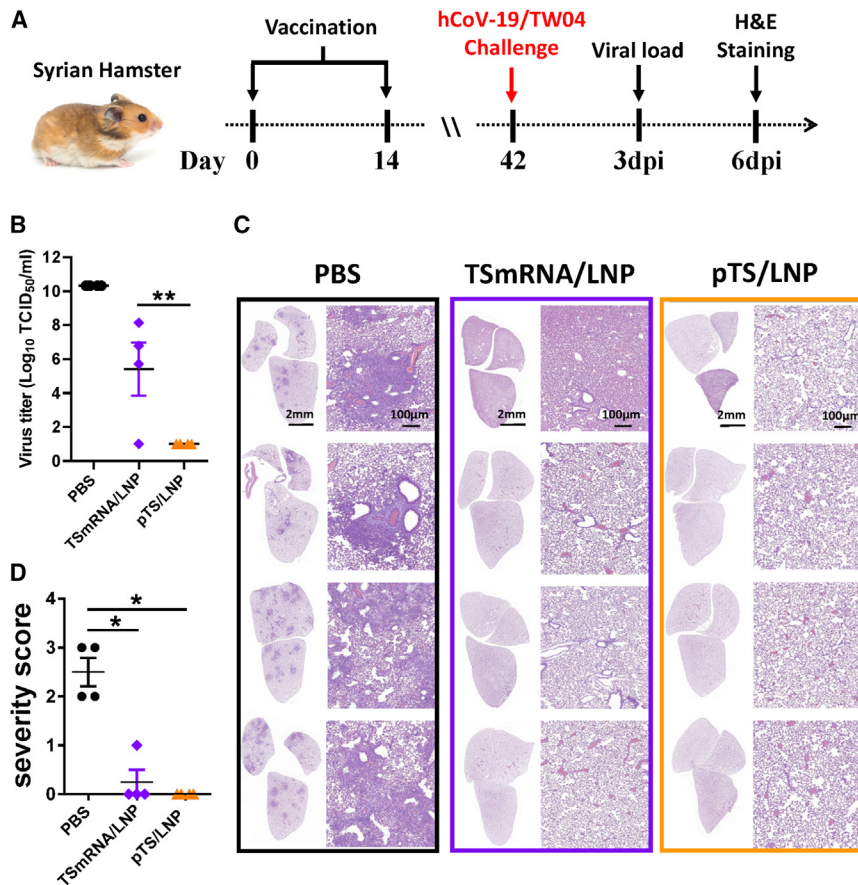


Figure 6. The pTS/LNP immunization provides full protection in hamster challenge model

(A) Schematic showing the schedule of animal study. Syrian hamsters (n = 8/group) were immunized with PBS as control, 10 μg TSmRNA/LNP, or 10 μg pTS/LNP at weeks 0 and 2. The immunized hamsters were challenged with SARS-CoV-2 TW04 via nasal inoculation at week 6. (B) Viral titers in the lungs of infected hamsters (n = 4/group) at 3 dpc were determined by TCID₅₀ assay. (C) Histopathology of lungs from infected hamsters (n = 4/group) at 6 dpc was performed by hematoxylin and eosin staining. Scale bar for the low-magnification image, 2 mm; scale bar for the high-magnification image, 100 μm. (D) Pathological severity scores of lung tissue from infected hamsters. The p value was calculated by Mann-Whitney test. *p < 0.05 and **p < 0.008.

(Figures 3D and 4D) and neutralizing antibodies (Figures 4E and 4F) in hamsters.

The level of antigen expression and the accessibility of the antigen to the immune system are two aspects that can be considered when discussing the different responses observed in model animals. The amount of antigen produced after DNA/LNP injection is mainly determined by the amount of DNA introduced into cells. Gene transfer using plasmid DNA has been reported to be most efficient in skeletal muscle.⁴⁰ However, intramuscular immunization of DNA vaccines induces immunity that varies depending on the injection sites.

For example, injection of plasmid DNA into the tibialis anterior muscle induced a humoral response stronger than that of the quadriceps muscle.⁴¹ The immune responses to the encoded antigen may be affected by several factors that influence the uptake and expression of plasmid DNA in skeletal muscle. For example, muscle fibers are surrounded by connective tissues, which vary between different types of skeletal muscle and may affect the diffusion of DNA within the muscle tissue or the uptake of DNA into muscle cells.⁴² It is speculated that the muscle structure of the hamster hindlimb may be more conducive for plasmid DNA to access the muscle fiber nucleus than that of other species, resulting in a greater amount of antigen expression. Therefore, immune responses elicited by DNA/LNP are superior to those induced by mRNA/LNP in hamsters, but not in mice, rats, or rabbits. In addition, another possible explanation for this intriguing finding in hamsters is that the preference of CpG motifs for Toll-like receptor 9 (TLR9) stimulation varies across species.⁴³ It is well known that the optimal CpG motifs differ between mice and humans,^{44,45} but there is little information regarding which TLR9 agonist sequences are preferred in hamsters. These findings suggest that DNA/LNP immunogenicity may be species dependent. Therefore, differences in immune responses between species may need to be considered in the evaluation of nucleic acid vaccines, especially when comparing DNA and mRNA vaccines

year.^{38,39} Successful DNA vaccines can be delivered to any region of the world, including low- and middle-income countries. Our report showed that DNA/LNPs are feasible for a new-generation COVID-19 vaccine that can efficiently induce antiviral immunity in animals. In mice, 2 μg pTS/LNP immunization induced anti-TS antibody titers similar to those induced by 20 μg pTS DNA with electroporation and higher than those induced by 20 μg naked pTS DNA immunization (Figure 1B). Accordingly, 2 μg pTS/LNP immunization induced a level of neutralizing antibodies against SARS-CoV-2 similar to 20 μg pTS DNA with electroporation and significantly higher than that with 20 μg naked pTS DNA immunization (Figure 1C).

When comparing the immunogenicity of mRNA/LNPs and DNA/LNPs vaccinations in different animals, we discovered that the effects of DNA/LNPs varied between animal species. After prime and boost regimens, the DNA/LNP immunization generally induced antigen-specific antibody response comparable with mRNA/LNP in mice, rats, and rabbits (Figure 3). Four weeks after the second vaccination, pTS/LNP immunized mice showed a lower spike-binding antibody than those from TSmRNA/LNP group (Figure 4A); however, similar neutralizing antibody titers (Figures 4B and 4C) were detected in serum of both groups. Interestingly, DNA/LNP immunization significantly increased the titers of both anti-TS antibodies

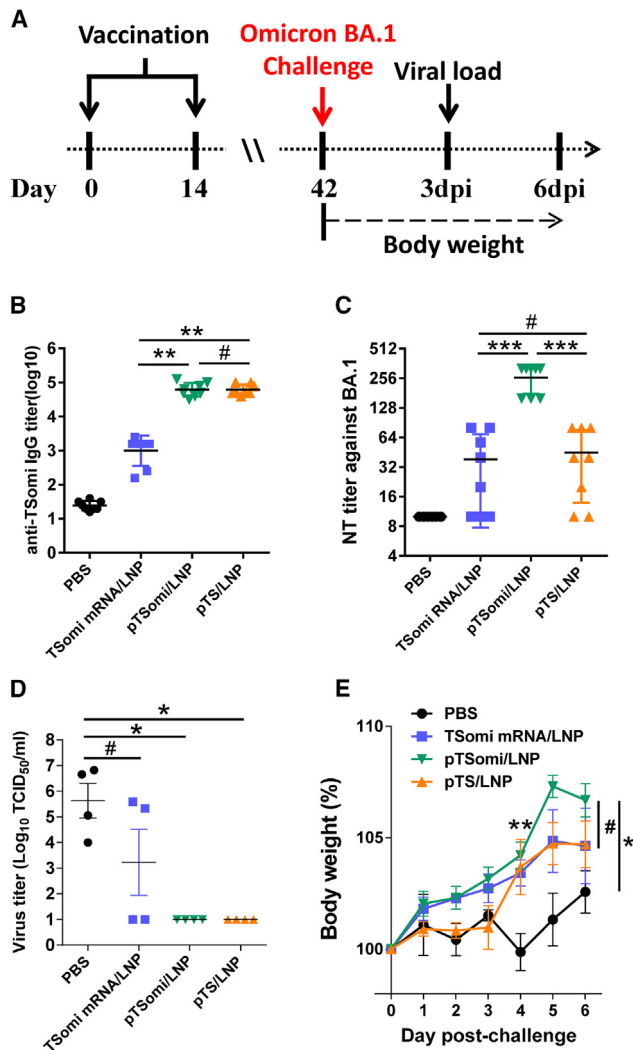


Figure 7. pTS/LNP immunization can even elicit effective immunity against the Omicron BA.1 variant in hamsters

(A) Schematic showing the schedule of animal study. Syrian hamsters ($n = 8/\text{group}$) were immunized with PBS, 2 μg TSomi mRNA/LNP, 2 μg pTSomi DNA/LNP, or 2 μg pTS/LNP at weeks 0 and 2. The sera collected from these hamsters at week 6 were used to determine (B) the spike-specific IgG titers by antigen-coating ELISA and to analyze (C) the neutralizing titers by TCID₅₀ assay. The immunized hamsters were challenged with SARS-CoV-2 Omicron BA.1 TW/16804 via nasal inoculation at week 6. (D) Viral titers in the lungs of infected hamsters ($n = 4/\text{group}$) at 3 dpc were determined by TCID₅₀ assay. The p value was calculated by Mann-Whitney test. * $p < 0.05$ and ** $p < 0.008$; # Not significant. (E) Body weight change (%) of the infected hamsters ($n = 4/\text{group}$) was daily recorded until dpc 6. The p value was calculated by two-way ANOVA. * $p < 0.05$ and ** $p < 0.008$. ns, not significant.

in preclinical studies. In addition, understanding why DNA/LNPs are superior to mRNA/LNPs in hamsters could be useful in the future development of nucleic acid vaccines. Since we have shown potential of DNA/LNPs vaccination, these results may provide a new insight for next-generation vaccine development. Furthermore, clinical data of DNA/LNPs immunization are critical in future applications.

In addition, we compared the T cell responses elicited by vaccination with DNA/LNP, mRNA/LNP, and recombinant protein formulated with aluminum adjuvant. Aluminum hydroxide is a well-known Th2-biased adjuvant that promotes the production of high levels of the Th2 cytokines IL-5 and IL-13, which were shown to be significantly lower in the mRNA/LNP and DNA/LNP vaccinated groups (Figures 5C and 5D). Since mRNA/LNP has been documented to induce Th1/Th2-balanced immune responses,^{46,47} the ratios of Th1/Th2 cytokines were not high after recombinant spike protein stimulation in the mRNA/LNP immunization group (Figures 5E and 5F). Although the pTS/LNP vaccine elicited a relatively low IFN- γ and IL-2 response when compared with the TSmRNA/LNP vaccine in mice 1 week after the booster, the DNA/LNP vaccine elicited Th1-biased immune responses similar to those induced by naked DNA vaccination.^{14,48} In hamsters, cellular immunity was also observed with a greater preference for Th1 responses in the DNA/LNP vaccinated group than mRNA/LNP group (Figure S3). The Th1-biased immune responses can induce the production of higher levels of cytotoxic T cells, which are important for virus clearance^{49,50} and tumor killing.^{51–53}

mRNA/LNP vaccines against COVID-19 have been shown to induce potent immunity to protect hamsters from viral infection.^{54–56} Interestingly, DNA/LNP immunization provided greater protection than mRNA/LNP immunization in hamsters challenged with SARS-CoV-2 Wuhan strain (Figure 6) and Omicron BA.1 (Figure 7). At 3 dpc, mRNA/LNPs partially inhibited viral replication in the lung of hamsters, whereas there was no detectable viral load in the lung of DNA/LNP-immunized hamsters (Figures 6B and 7D), despite the fact that pTS/LNPs did not induce neutralizing antibodies against Omicron BA.1 as effectively as pTSomi/LNPs (Figure 7C). The inflammation in the lung after virus challenge was still mild in the mRNA/LNP immunization group, but there was no inflammation observed in the DNA/LNP immunization group (Figures 6C and 6D). The results were better than those for previously reported DNA vaccines in hamsters.^{14,57,58}

There are some limitations to this study. We mainly compared the immunogenicity of mRNA/LNP and DNA/LNP by evaluating humoral responses and neutralizing antibodies, which are the most important criteria for prophylactic vaccines. DNA-based vaccines are also able to induce robust cytotoxic T lymphocyte response to eliminate infected cells by recognizing spike-specific epitopes.^{59,60} Mutations emerging on the spike of variants can easily escape from antibody neutralization, whereas most linear T cell epitopes are conserved in VOCs.^{54,61} However, due to the scarcity of hamster-specific antibodies developed for immunological research, we could not comprehensively investigate the differences in vaccine-induced cell-mediated immunity between mRNA/LNPs and DNA/LNPs in hamsters. In vaccine safety assessment, 10 μg and 50 μg DNA/LNPs and mRNA/LNPs were used to compare their effects on hamsters and rabbits, respectively. Either injected by DNA/LNPs or mRNA/LNPs, we did not observe abnormal physiologic changes in animals. However, the DNA/LNP vaccine platform still needs more safety testing before going into clinical trials.

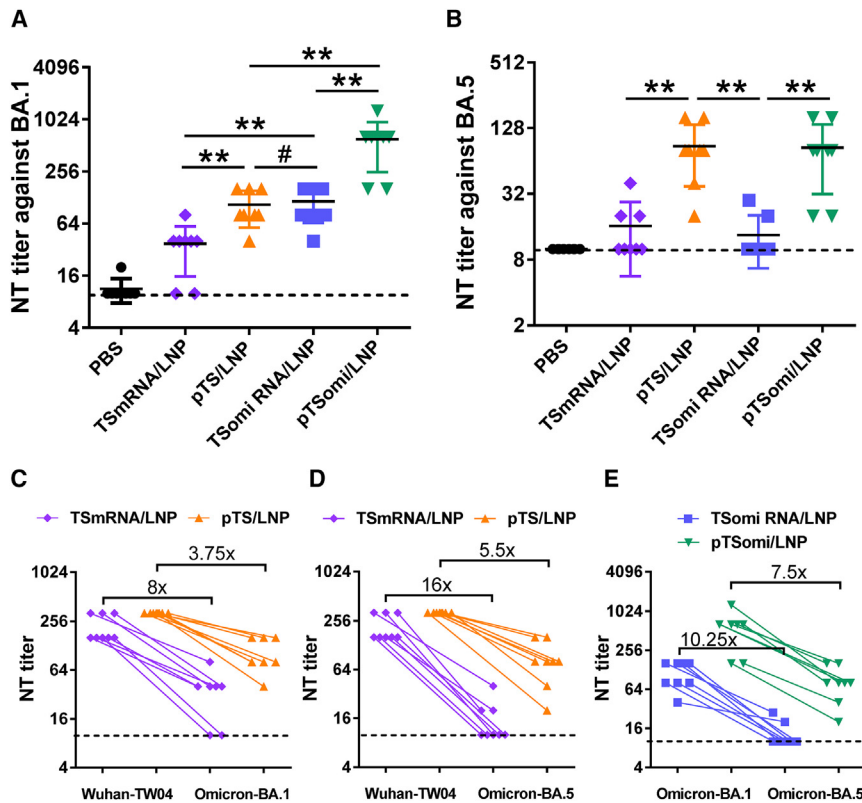


Figure 8. The pDNA/LNP immunization induces higher cross-neutralization titers than mRNA/LNP

Syrian hamsters ($n = 8/\text{group}$) were immunized with $10 \mu\text{g}$ of indicated vaccine at weeks 0 and 2. Serum collected at week 6 was used to determine neutralizing titers against (A) Omicron BA.1 and (B) BA.5 variants by TCID_{50} assay. (C–E) The pairwise comparisons of the NT titers between Wuhan-TW04, Omicron BA.1, or Omicron BA.5. Each symbol represents an individual hamster. Each line links two symbols of the same hamster, which represents NT titers measured by two VOCs neutralization assays. The numbers above the brackets are the average reduction fold of the NT titers between two indicated virus strains. Dash lines indicate the limited NT titers of detection of 10. The p value was calculated by Mann-Whitney test. * $p < 0.05$ and ** $p < 0.008$ were considered significant, # Not significant.

Although mRNA vaccines have recently emerged as an appealing alternative to DNA vaccines for COVID-19, the thermal instability of mRNA vaccines is the major obstacle to global delivery. The high thermostability and easy manufacturing process are attractive for developing efficient DNA delivery. The optimal LNP compositions for DNA delivery are still under investigation.³⁴ In particular, Mucker et al.³⁵ reported that DNA formulated with their lipid delivery technology platform LNUAR generates >10-fold increased neutralizing antibody titers while utilizing 10 times less DNA than naked DNA in trans-chromosome bovines. They found that 1 mg DNA/LNP vaccination yielded similar levels of neutralizing antibody compared with 0.1 mg/DNA/LNP vaccination, and the reactogenicity of 1 mg of DNA/LNP was higher than 0.1 mg DNA/LNP. However, the current investigation of DNA/LNPs remains limited. The LNP formulation for DNA delivery is important for filling the gap left by the mRNA vaccine; thus, the safe and optimal LNP compositions for DNA delivery may need to be studied intensively in the future.

MATERIALS AND METHODS

Plasmid construction

The DNA vaccine construct expressing the SARS-CoV-2 spike protein was constructed by insertion of the full-length spike protein sequence into the *NheI* and *NotI* cloning sites of pVAX1 (Thermo Fisher Scientific).¹⁵ To stabilize the SARS-CoV-2 S protein in the prefusion state, a pVAX-TS (pTS) construct was designed to encode a TS sequence that contains a “GSAS” replacement at the

sequence on the pT7ts plasmid (Addgene) was used as the template for TS (or TSomi) mRNA *in vitro* transcription.

mRNA synthesis

The pT7TS plasmid was linearized for 4 h with the restriction enzyme *SmaI* (Fermentas) as a DNA template for mRNA *in vitro* transcription. The linearized pT7TS DNA in $200 \mu\text{L}$ was recovered by precipitating it with $40 \mu\text{L}$ 5 M NaOAc (Invitrogen) and $480 \mu\text{L}$ 100% EtOH, followed by 30 min of chilling at -20°C . The linearized pT7TS DNA was washed twice with 1 mL 75% EtOH after being centrifuged at 15,000 rpm for 20 min at 4°C . Following air drying, pT7TS DNA was resuspended to $1 \mu\text{g}/\mu\text{L}$ in H_2O (Sigma). A single *in vitro* transcription reaction of TS mRNA in $40 \mu\text{L}$ contained $1 \mu\text{g}$ pT7TS DNA as a template, 5 mM guanosine triphosphate, ATP, cytidine triphosphate, and N1-methyl-pseudoUTP (TriLink, San Diego), 4 mM CleanCap AG 3'Ome, 0.002 U/ μL pyrophosphatase (Thermo Fisher Scientific), 1 U RNase inhibitor, and 10 U/ μL T7 polymerase; the reaction was incubated for 90 min at 37°C . The TS mRNA was isolated from the *in vitro* transcription reaction by using a MegaClear RNA purification kit (Thermo Fisher Scientific) and resuspended in H_2O for LNP preparation.

LNP preparation

We purchased 8-[(2-hydroxyethyl) [6-oxo-6-(undecyloxy)hexyl] amino]-octanoic acid and 1-octylnonyl ester (SM-102) in chloroform

from Cayman Chemical Company. We purchased 1,2-Distearoyl-sn-glycero-3-phosphocholine (DSPC), cholesterol and 1,2-dimyristoyl-rac-glycero-3-methoxypolyethylene glycol-2000 (DMG-PEG) from Merck. The pDNA/LNP and mRNA/LNP formulations were prepared using a modified version of a previously described method.⁵⁴ Briefly, lipids were dissolved in ethanol at molar ratios of 50:10:38.5:1.5 (SM-102: DSPC: cholesterol: DMG-PEG). The lipid mixture was combined with an acidification buffer (25 mM sodium acetate [pH 5.0]) containing pDNA or mRNA at a volume ratio of 3:1 (aqueous: ethanol) using a microfluidic mixer (Precision Nanosystems). The lipid nitrogen-to-phosphate ratio was set to 6. Formulations were diluted 40 times with 20 mM Tris (pH 7.4) and then further concentrated using Amicon ultracentrifugal filters (EMD Millipore). The mRNA-LNP formulations were passed through a 0.45- μ m filter before administration. The formulated pDNA/LNP and mRNA/LNP were characterized for parameters such as encapsulation efficiency, particle size distribution, and polydispersity index (Table S1).

Animal study

BALB/c mice, Sprague-Dawley rats, golden Syrian hamsters, and New Zealand rabbits were obtained from the National Laboratory Animal Breeding and Research Center or BioLASCO Co., Ltd. Mice, hamsters, and Sprague-Dawley rats were used between 6 and 20 weeks of age. Anesthetized mice were vaccinated with a 50 μ L of a solution containing 2 μ g pDNA/LNP or mRNA/LNP through injection in the gastrocnemius muscle at the hindlimb. Blood samples of mice were collected by submandibular vein blood sampling. Anesthetized hamsters and Sprague-Dawley rats were vaccinated with 100 μ L solution containing the indicated dosage (2 μ g or 10 μ g) pDNA/LNP or mRNA/LNP through intramuscular injection at hindlimb. Blood samples of hamsters and rats were collected by gingival and tail vein blood sampling, respectively. All animals were kept at the Animal Center of the National Health Research Institutes (NHRI) and maintained according to institutional animal care protocols. The animal experimental protocols were approved by the Institutional Animal Care and Use Committee (IACUC) of the NHRI (protocol Nos.: NHRI-IACUC-109077-A and NHRI-IACUC-110053-A).

Antibody titration

The antigen-specific antibodies from immunized animals against the recombinant trimeric (TS) protein were quantified by using ELISA. Briefly, 100 μ L 4 μ g/mL recombinant SARS-CoV-2 TS protein in 0.1 M carbonate buffer (pH 9.5) was coated onto 96-well microplates by overnight incubation at 4°C. The TS protein-coated plates were washed twice with 0.05% Tween 20 in PBS (PBS-T) and then blocked with 3% BSA in PBS at room temperature for 1 h. The serially diluted serum from immunized animals was transferred into the plates, which were incubated for another 2 h at room temperature. After washing the plates with PBS-T, horseradish peroxidase (HRP)-conjugated rabbit anti-hamster IgG (cat# ARG23730, Arigo Bio-laboratories), HRP-conjugated goat anti-mouse IgG (Thermo Fisher Scientific), HRP-conjugated goat anti-rat IgG (Bethyl Laboratories),

or HRP-conjugated goat anti-rabbit IgG (cat# ARG23768, Arigo Bio-laboratories) was used as the secondary antibody. The assay was developed by using TMB substrate (Biolegend). The absorbance was measured by an ELISA reader at 450 nm.

Neutralization assay

The day before neutralization assays were conducted, Vero cells (2.4×10^4 cells/well) were seeded in 96-well plates to develop a monolayer. Heat-labile nonspecific viral inhibitory substances were inactivated in antisera obtained from immunized animals by heating at 56°C for 30 min. The serum was diluted to a starting concentration of 1/20 with M199 medium (Gibco), added to a well containing 200 TCID₅₀ of SARS-CoV-2 in 0.2 mL, and incubated at 37°C for 2 h. Next, the virus-serum blends were transferred to 96-well plates with a monolayer of Vero cells and incubated at 37°C. Each serum dilution was tested four times in quadruplicate. After 4–5 days of incubation, the cytopathic effect in each well was defined. The neutralization titer corresponded to the greatest serum dilution that inhibited infection in 50% of quadruplicate inoculations. For calculations, neutralization titers below the 1:20 initial dilution were given a value of 10.

Cytokine measurements

The production of cytokines by splenocytes was assessed using a cytokine ELISA. Two weeks after the second vaccination, spleens were harvested from individual mice in each group. Splenocytes were obtained from mesh-homogenized spleens in RPMI-1640 medium and suspended in LCM containing 10% fetal bovine serum. The splenocytes were cultured with recombinant SARS-CoV-2 TS protein (5 μ g/mL) at 37°C and with 5% CO₂ in 24-well plates containing 5×10^5 cells per well. After 3 days, the culture supernatant was collected to determine the levels of Th1 cytokines (IFN- γ and IL-2) and Th2 cytokines (IL-5 and IL-13) using individual cytokine ELISA kits (Invitrogen) according to the instructions provided by the manufacturer.

Viral challenge

Syrian hamsters (n = 8 per group) were immunized with 10 μ g mRNA/LNP or pDNA/LNP at weeks 0 and 2 via i.m. injection. Three weeks after the second vaccination, these hamsters were challenged intranasally with 1×10^4 TCID₅₀ of SARS-CoV-2 (hCoV-19/Taiwan/4/2020) or 2×10^4 TCID₅₀ of SARS-CoV-2 Omicron BA.1 variant (hCoV-19/Taiwan/16804/2021) in a volume of 50 μ L under isoflurane anesthesia. The daily body weight changes of infected hamsters (n = 4 per group) were monitored until 6 dpc. At 3 dpc, four infected hamsters from each group were sacrificed for viral load analysis. To evaluate the viral load in the lung, left lung tissues were homogenized in 2 mL PBS using a MACS Dissociator (Miltenyi Biotec). Following 5 min of centrifugation at 600 \times g, the cleared supernatant was collected for live virus titration (TCID₅₀ assay).

Histochemistry

Lung tissue samples from infected hamsters were formalin fixed, dehydrated, and then paraffin embedded. The wax-embedded tissue

blocks were sliced into 4- μ m sections and stained with hematoxylin and eosin for pathological assessment. The lung pathology was categorized as pulmonary consolidation, edema, peribronchiolitis, perivascularitis, and alveolitis, which were evaluated by a clinical pathologist at the NHRI core pathology facility. Pathological scores based on the criterion described in a previous study³⁶ were used to quantify the severity of lung tissue lesions. Each animal was assigned a sum score based on all of the images of the lobes.

Live animal luminescence imaging

BALB/c mice (n = 4 per group) were administered with 2 μ g and 10 μ g CBGr99 encoding mRNA or pDNA encapsulated within LNPs via the i.m. injection in the thigh muscles of the hindlimb. For the bioluminescence imaging at the indicated time points, the mice were intraperitoneally (i.p.) injected with the luciferase substrate luciferin (150 mg/kg, Abcam). After performing 11 min for luciferin distribution to the target site, mice were transferred into the IVIS Spectrum instrument's imaging chamber for luminescence signals collection. The luminescence or fluorescence intensities in each region of interest were quantified using the Living Image 3.0 software (PerkinElmer).

Statistics

All data were statistically analyzed using GraphPad Prism software. The statistical significance of the mean value between two experimental groups was determined by the two-tailed Mann-Whitney test. A two-way ANOVA was applied for multiple groups at different time points; p values of less than 0.05 were considered significant, and ns indicates not significant.

DATA AND CODE AVAILABILITY

The findings of this study are available within this paper or are available from the corresponding author upon reasonable request.

SUPPLEMENTAL INFORMATION

Supplemental information can be found online at <https://doi.org/10.1016/j.omtm.2023.101169>.

ACKNOWLEDGMENTS

We acknowledge the Centers for Disease Control and the Ministry of Health and Welfare for providing SARS-CoV-2 and the ABSL3 team of the NHRI for handling the virus in this study. We also thank the Laboratory Animal Center and Pathology Core Laboratory of the NHRI for technical support. This study was funded by the Ministry of Health and Welfare (No. MOHW110-TDU-C-222-000010 to L.C.L.) and the NHRI of Taiwan (IV-110-GP-05 and IV-111-GP-06 to S.J.L. and 111A1-IVPP-02 to M.H.H.).

AUTHOR CONTRIBUTIONS

H.C.L., K.Y.S., C.H.Y., M.H.H., and S.J.L. designed the experiments, analyzed the data, and prepared the manuscript; H.W.C. and C.L.L. aided in the manuscript review; W.C.H., F.F.C., K.Y.S., C.H.Y., H.M.H., and C.Y.H. performed the experiments; Y.H.C., H.W.C., and H.C.L. developed reagents; C.L.L., H.W.C., M.H.H., and S.J.L.

provided supervision and oversaw the final manuscript preparation; K.Y.S., H.C. L., and S.J.L. wrote the paper.

DECLARATION OF INTERESTS

The authors have no conflicts of interest to declare.

REFERENCES

- Liu, J., Wu, J., Wang, B., Zeng, S., Qi, F., Lu, C., Kimura, Y., and Liu, B. (2014). Oral vaccination with a liposome-encapsulated influenza DNA vaccine protects mice against respiratory challenge infection. *J. Med. Virol.* 86, 886–894.
- Tian, M., Zhou, Z., Tan, S., Fan, X., Li, L., and Ullah, N. (2018). Formulation in DDA-MPLA-TDB Liposome Enhances the Immunogenicity and Protective Efficacy of a DNA Vaccine against Mycobacterium tuberculosis Infection. *Front. Immunol.* 9, 310.
- Zhang, M., Hong, Y., Chen, W., and Wang, C. (2017). Polymers for DNA Vaccine Delivery. *ACS Biomater. Sci. Eng.* 3, 108–125.
- Karpenko, L.I., Apartsin, E.K., Dudko, S.G., Starostina, E.V., Kaplina, O.N., Antonets, D.V., Volosnikova, E.A., Zaitsev, B.N., Bakulina, A.Y., Venyaminova, A.G., et al. (2020). Cationic Polymers for the Delivery of the Ebola DNA Vaccine Encoding Artificial T-Cell Immunogen. *Vaccines* 8, 718.
- Colombani, T., Haudebourg, T., and Pitard, B. (2023). 704/DNA vaccines leverage cytoplasmic DNA stimulation to promote anti-HIV neutralizing antibody production in mice and strong immune response against alpha-fetoprotein in non-human primates. *Mol. Ther. Nucleic Acids* 32, 743–757.
- Dey, A., Chozhavel Rajanathan, T.M., Chandra, H., Pericherla, H.P.R., Kumar, S., Choonia, H.S., Bajpai, M., Singh, A.K., Sinha, A., Saini, G., et al. (2021). Immunogenic potential of DNA vaccine candidate, ZyCoV-D against SARS-CoV-2 in animal models. *Vaccine* 39, 4108–4116.
- Lin, C.T., Yen, C.F., Shaw, S.W., Yen, T.C., Chen, Y.J., Soong, Y.K., and Lai, C.H. (2009). Gene gun administration of therapeutic HPV DNA vaccination restores the efficacy of prolonged defrosted viral based vaccine. *Vaccine* 27, 7352–7358.
- Todorova, B., Adam, L., Culina, S., Boisgard, R., Martinon, F., Cosma, A., Ustav, M., Kortulewski, T., Le Grand, R., and Chapon, C. (2017). Electroporation as a vaccine delivery system and a natural adjuvant to intradermal administration of plasmid DNA in macaques. *Sci. Rep.* 7, 4122.
- Chen, H., Zheng, X., Wang, R., Gao, N., Sheng, Z., Fan, D., Feng, K., Liao, X., and An, J. (2016). Immunization with electroporation enhances the protective effect of a DNA vaccine candidate expressing prME antigen against dengue virus serotype 2 infection. *Clin. Immunol.* 171, 41–49.
- Wang, Q., Jiang, W., Chen, Y., Liu, P., Sheng, C., Chen, S., Zhang, H., Pan, C., Gao, S., and Huang, W. (2014). In vivo electroporation of minicircle DNA as a novel method of vaccine delivery to enhance HIV-1-specific immune responses. *J. Virol.* 88, 1924–1934.
- Mallapaty, S. (2021). India's DNA COVID vaccine is a world first - more are coming. *Nature* 597, 161–162.
- Sheridan, C. (2021). First COVID-19 DNA vaccine approved, others in hot pursuit. *Nat. Biotechnol.* 39, 1479–1482.
- Andrade, V.M., Christensen-Quick, A., Agnes, J., Tur, J., Reed, C., Kalia, R., Marrero, I., Elwood, D., Schultheis, K., Purwar, M., et al. (2021). INO-4800 DNA vaccine induces neutralizing antibodies and T cell activity against global SARS-CoV-2 variants. *NPJ Vaccines* 6, 121.
- Tzeng, T.T., Chai, K.M., Shen, K.Y., Yu, C.Y., Yang, S.J., Huang, W.C., Liao, H.C., Chiu, F.F., Dou, H.Y., Liao, C.L., et al. (2022). A DNA vaccine candidate delivered by an electrocupuncture machine provides protective immunity against SARS-CoV-2 infection. *NPJ Vaccines* 7, 60.
- Chai, K.M., Tzeng, T.T., Shen, K.Y., Liao, H.C., Lin, J.J., Chen, M.Y., Yu, G.Y., Dou, H.Y., Liao, C.L., Chen, H.W., and Liu, S.J. (2021). DNA vaccination induced protective immunity against SARS CoV-2 infection in hamsters. *PLoS Neglected Trop. Dis.* 15, e0009374.
- Gurwith, M.J., Horwith, G.S., Impellizzeri, C.A., Davis, A.R., Lubeck, M.D., and Hung, P.P. (1989). Current use and future directions of adenovirus vaccine. *Semin. Respir. Infect.* 4, 299–303.

17. Sasso, E., D'Alise, A.M., Zambrano, N., Scarselli, E., Folgori, A., and Nicosia, A. (2020). New viral vectors for infectious diseases and cancer. *Semin. Immunol.* *50*, 101430.
18. Mennechet, F.J.D., Paris, O., Ouoba, A.R., Salazar Arenas, S., Sirima, S.B., Takoudjou Dzomo, G.R., Diarra, A., Traore, I.T., Kania, D., Eichholz, K., et al. (2019). A review of 65 years of human adenovirus seroprevalence. *Expert Rev. Vaccines* *18*, 597–613.
19. Voysey, M., Clemens, S.A.C., Madhi, S.A., Weckx, L.Y., Folegatti, P.M., Aley, P.K., Angus, B., Baillie, V.L., Barnabas, S.L., Bhorat, Q.E., et al. (2021). Safety and efficacy of the ChAdOx1 nCoV-19 vaccine (AZD1222) against SARS-CoV-2: an interim analysis of four randomised controlled trials in Brazil, South Africa, and the UK. *Lancet* *397*, 99–111.
20. GOV.UK (2020). Regulatory Approval of COVID-19 Vaccine AstraZeneca. <https://www.gov.uk/government/publications/regulatory-approval-of-covid-19-vaccine-astrazeneca>.
21. Halperin, S.A., Ye, L., MacKinnon-Cameron, D., Smith, B., Cahn, P.E., Ruiz-Palacios, G.M., Ikram, A., Lanas, F., Lourdes Guerrero, M., Muñoz Navarro, S.R., et al. (2022). Final efficacy analysis, interim safety analysis, and immunogenicity of a single dose of recombinant novel coronavirus vaccine (adenovirus type 5 vector) in adults 18 years and older: an international, multicentre, randomised, double-blinded, placebo-controlled phase 3 trial. *Lancet* *399*, 237–248.
22. WHO (2022). Interim Recommendations for Use of the Cansino Ad5-nCoV-S Vaccine (Convidecia ®) against COVID-19. <https://www.who.int/publications/item/WHO-2019-nCoV-vaccines-SAGE-recommendation-Ad5-nCoV-Convidecia>.
23. FDA.US (2021). FDA Issues Emergency Use Authorization for Third COVID-19 Vaccine. <https://www.fda.gov/news-events/press-announcements/fda-issues-emergency-use-authorization-third-covid-19-vaccine>.
24. Sadoff, J., Gray, G., Vandebosch, A., Cárdenas, V., Shukarev, G., Grinsztejn, B., Goepfert, P.A., Truyers, C., Van Dromme, I., Spiessens, B., et al. (2022). Final Analysis of Efficacy and Safety of Single-Dose Ad26. *N. Engl. J. Med.* *386*, 847–860.
25. Shirley, J.L., de Jong, Y.P., Terhorst, C., and Herzog, R.W. (2020). Immune Responses to Viral Gene Therapy Vectors. *Mol. Ther.* *28*, 709–722.
26. Shah, M.A.A., He, N., Li, Z., Ali, Z., and Zhang, L. (2014). Nanoparticles for DNA vaccine delivery. *J. Biomed. Nanotechnol.* *10*, 2332–2349.
27. Shah, M.A.A., Ali, Z., Ahmad, R., Qadri, I., Fatima, K., and He, N. (2015). DNA Mediated Vaccines Delivery Through Nanoparticles. *J. Nanosci. Nanotechnol.* *15*, 41–53.
28. Mainini, F., and Eccles, M.R. (2020). Lipid and Polymer-Based Nanoparticle siRNA Delivery Systems for Cancer Therapy. *Molecules* *25*, 2692.
29. Akinc, A., Maier, M.A., Manoharan, M., Fitzgerald, K., Jayaraman, M., Barros, S., Ansell, S., Du, X., Hope, M.J., Madden, T.D., et al. (2019). The Onpatro story and the clinical translation of nanomedicines containing nucleic acid-based drugs. *Nat. Nanotechnol.* *14*, 1084–1087.
30. Gilleron, J., Querbes, W., Zeigerer, A., Borodovsky, A., Marsico, G., Schubert, U., Manygoats, K., Seifert, S., Andree, C., Stöter, M., et al. (2013). Image-based analysis of lipid nanoparticle-mediated siRNA delivery, intracellular trafficking and endosomal escape. *Nat. Biotechnol.* *31*, 638–646.
31. Wang, Y., and Huang, L. (2013). A window onto siRNA delivery. *Nat. Biotechnol.* *31*, 611–612.
32. Algarni, A., Pilkington, E.H., Suys, E.J.A., Al-Wassiti, H., Pouton, C.W., and Truong, N.P. (2022). In vivo delivery of plasmid DNA by lipid nanoparticles: the influence of ionizable cationic lipids on organ-selective gene expression. *Biomater. Sci.* *10*, 2940–2952.
33. Zhu, Y., Shen, R., Vuong, I., Reynolds, R.A., Shears, M.J., Yao, Z.C., Hu, Y., Cho, W.J., Kong, J., Reddy, S.K., et al. (2022). Multi-step screening of DNA/lipid nanoparticles and co-delivery with siRNA to enhance and prolong gene expression. *Nat. Commun.* *13*, 4282.
34. Quagliarini, E., Wang, J., Renzi, S., Cui, L., Digiacomo, L., Ferri, G., Pesce, L., De Lorenzi, V., Matteoli, G., Amenitsch, H., et al. (2022). Mechanistic Insights into the Superior DNA Delivery Efficiency of Multicomponent Lipid Nanoparticles: An In Vitro and In Vivo Study. *ACS Appl. Mater. Interfaces* *14*, 56666–56677.
35. Mucker, E.M., Karmali, P.P., Vega, J., Kwilas, S.A., Wu, H., Joselyn, M., Ballantyne, J., Sampey, D., Mukthavaram, R., Sullivan, E., et al. (2020). Lipid Nanoparticle Formulation Increases Efficiency of DNA-Vectored Vaccines/Immunoprophylaxis in Animals Including Transchromosomal Bovines. *Sci. Rep.* *10*, 8764.
36. Liao, H.C., Wu, W.L., Chiang, C.Y., Huang, M.S., Shen, K.Y., Huang, Y.L., Wu, S.C., Liao, C.L., Chen, H.W., and Liu, S.J. (2022). Low-Dose SARS-CoV-2 S-Trimer with an Emulsion Adjuvant Induced Th1-Biased Protective Immunity. *Int. J. Mol. Sci.* *23*, 4902.
37. Corbett, K.S., Edwards, D., Leist, S.R., Abiona, O.M., Boyoglu-Barnum, S., Gillespie, R.A., Himansu, S., Schäfer, A., Ziwawo, C.T., DiPiazza, A.T., et al. (2020). SARS-CoV-2 mRNA Vaccine Development Enabled by Prototype Pathogen Preparedness. Preprint at bioRxiv. <https://doi.org/10.1101/2020.06.11.145920>.
38. Kutzler, M.A., and Weiner, D.B. (2008). DNA vaccines: ready for prime time? *Nat. Rev. Genet.* *9*, 776–788.
39. Van Damme, P., Cramm, M., Safary, A., Vandepapelière, P., and Meheus, A. (1992). Heat stability of a recombinant DNA hepatitis B vaccine. *Vaccine* *10*, 366–367.
40. Davis, H.L., Whalen, R.G., and Demeneix, B.A. (1993). Direct gene transfer into skeletal muscle *in vivo*: factors affecting efficiency of transfer and stability of expression. *Hum. Gene Ther.* *4*, 151–159.
41. Yokoyama, M., Hassett, D.E., Zhang, J., and Whitton, J.L. (1997). DNA immunization can stimulate florid local inflammation, and the antiviral immunity induced varies depending on injection site. *Vaccine* *15*, 553–560.
42. Davis, H.L., Michel, M.L., and Whalen, R.G. (1995). Use of plasmid DNA for direct gene transfer and immunization. *Ann. N. Y. Acad. Sci.* *772*, 21–29.
43. Roberts, T.L., Sweet, M.J., Hume, D.A., and Stacey, K.J. (2005). Cutting edge: species-specific TLR9-mediated recognition of CpG and non-CpG phosphorothioate-modified oligonucleotides. *J. Immunol.* *174*, 605–608.
44. Bauer, S., Kirschning, C.J., Häcker, H., Redecke, V., Hausmann, S., Akira, S., Wagner, H., and Lipford, G.B. (2001). Human TLR9 confers responsiveness to bacterial DNA via species-specific CpG motif recognition. *Proc. Natl. Acad. Sci. USA* *98*, 9237–9242.
45. Liu, J., Xu, C., Liu, Y.L., Matsuo, H., Hsieh, R.P.F., Lo, J.F., Tseng, P.H., Yuan, C.J., Luo, Y., Xiang, R., and Chuang, T.H. (2012). Activation of rabbit TLR9 by different CpG-ODN optimized for mouse and human TLR9. *Comp. Immunol. Microbiol. Infect. Dis.* *35*, 443–451.
46. Corbett, K.S., Edwards, D.K., Leist, S.R., Abiona, O.M., Boyoglu-Barnum, S., Gillespie, R.A., Himansu, S., Schäfer, A., Ziwawo, C.T., DiPiazza, A.T., et al. (2020). SARS-CoV-2 mRNA vaccine design enabled by prototype pathogen preparedness. *Nature* *586*, 567–571.
47. Salleh, M.Z., Norazmi, M.N., and Deris, Z.Z. (2022). Immunogenicity mechanism of mRNA vaccines and their limitations in promoting adaptive protection against SARS-CoV-2. *PeerJ* *10*, e13083.
48. Kayraklioglu, N., Horuluoglu, B., and Klinman, D.M. (2021). CpG Oligonucleotides as Vaccine Adjuvants. *Methods Mol. Biol.* *2197*, 51–85.
49. Howard, F.H.N., Kwan, A., Winder, N., Mughal, A., Collado-Rojas, C., and Muthana, M. (2022). Understanding Immune Responses to Viruses-Do Underlying Th1/Th2 Cell Biases Predict Outcome? *Viruses* *14*.
50. Woodland, D.L., Hogan, R.J., and Zhong, W. (2001). Cellular immunity and memory to respiratory virus infections. *Immunol. Res.* *24*, 53–67.
51. Jäger, E., Jäger, D., and Knuth, A. (1999). CTL-defined cancer vaccines: perspectives for active immunotherapeutic interventions in minimal residual disease. *Cancer Metastasis Rev.* *18*, 143–150.
52. Weigelin, B., den Boer, A.T., Wagena, E., Broen, K., Dolstra, H., de Boer, R.J., Figdor, C.G., Textor, J., and Friedl, P. (2021). Cytotoxic T cells are able to efficiently eliminate cancer cells by additive cytotoxicity. *Nat. Commun.* *12*, 5217.
53. Yang, B., Jeang, J., Yang, A., Wu, T.C., and Hung, C.F. (2014). DNA vaccine for cancer immunotherapy. *Hum. Vaccines Immunother.* *10*, 3153–3164.
54. Shen, K.Y., Yang, C.H., Chen, C.T., Ho, H.M., Chiu, F.F., Huang, C.Y., Liao, H.C., Hsu, C.W., Yu, G.Y., Liao, C.L., et al. (2023). Omicron-specific mRNA vaccine induced cross-protective immunity against ancestral SARS-CoV-2 infection with low neutralizing antibodies. *J. Med. Virol.* *95*, e28370.
55. Hawman, D.W., Meade-White, K., Clancy, C., Archer, J., Hinkley, T., Leventhal, S.S., Rao, D., Stamper, A., Lewis, M., Rosenke, R., et al. (2022). Replicating RNA platform enables rapid response to the SARS-CoV-2 Omicron variant and elicits enhanced protection in naive hamsters compared to ancestral vaccine. *EBioMedicine* *83*, 104196.

56. Wu, Y., Shen, Y., Wu, N., Zhang, X., Chen, S., Yang, C., Zhou, J., Wu, Y., Chen, D., Wang, L., et al. (2022). Omicron-specific mRNA vaccine elicits potent immune responses in mice, hamsters, and nonhuman primates. *Cell Res.* 32, 949–952.
57. Babuadze, G.G., Fausther-Bovendo, H., deLaVega, M.A., Lillie, B., Naghibosadat, M., Shahhosseini, N., Joyce, M.A., Saffran, H.A., Lorne Tyrrell, D., Falzarano, D., et al. (2022). Two DNA vaccines protect against severe disease and pathology due to SARS-CoV-2 in Syrian hamsters. *NPJ Vaccines* 7, 49.
58. Brocato, R.L., Kwilas, S.A., Kim, R.K., Zeng, X., Principe, L.M., Smith, J.M., and Hooper, J.W. (2021). Protective efficacy of a SARS-CoV-2 DNA vaccine in wild-type and immunosuppressed Syrian hamsters. *NPJ Vaccines* 6, 16.
59. Conforti, A., Marra, E., Palombo, F., Roscilli, G., Ravà, M., Fumagalli, V., Muzi, A., Maffei, M., Luberto, L., Lione, L., et al. (2022). COVID-eVax, an electroporated DNA vaccine candidate encoding the SARS-CoV-2 RBD, elicits protective responses in animal models. *Mol. Ther.* 30, 311–326.
60. Tebas, P., Yang, S., Boyer, J.D., Reuschel, E.L., Patel, A., Christensen-Quick, A., Andrade, V.M., Morrow, M.P., Kraynyak, K., Agnes, J., et al. (2021). Safety and immunogenicity of INO-4800 DNA vaccine against SARS-CoV-2: A preliminary report of an open-label, Phase 1 clinical trial. *EClinicalMedicine* 31, 100689.
61. Redd, A.D., Nardin, A., Kared, H., Bloch, E.M., Abel, B., Pekosz, A., Laeyendecker, O., Fehlings, M., Quinn, T.C., and Tobian, A.A.R. (2022). Minimal Crossover between Mutations Associated with Omicron Variant of SARS-CoV-2 and CD8(+) T-Cell Epitopes Identified in COVID-19 Convalescent Individuals. *mBio* 13, e0361721.